

Phenomenology of Sterile Neutrinos

Carlo Giunti

INFN, Sezione di Torino, Via P. Giuria 1, I-10125 Torino, Italy

E-mail: giunti@to.infn.it

Abstract. The indications in favor of short-baseline neutrino oscillations, which require the existence of one or more sterile neutrinos, are reviewed. In the framework of 3+1 neutrino mixing, which is the simplest extension of the standard three-neutrino mixing which can partially explain the data, there is a strong tension in the interpretation of the data, mainly due to an incompatibility of the results of appearance and disappearance experiments. In the framework of 3+2 neutrino mixing, CP violation in short-baseline experiments can explain the difference between MiniBooNE neutrino and antineutrino data, but the tension between the data of appearance and disappearance experiments persists because the short-baseline disappearance of electron antineutrinos and muon neutrinos compatible with the LSND and MiniBooNE antineutrino appearance signal has not been observed.

Invited paper to NUFACT 11, XIIIth International Workshop on Neutrino Factories, Super beams and Beta beams, 1-6 August 2011, CERN and University of Geneva (Submitted to IOP conference series).

1. Introduction

From the results of solar, atmospheric and long-baseline neutrino oscillation experiments we know that neutrinos are massive and mixed particles (see Ref. [1]). There are two groups of experiments which measured two independent squared-mass differences (Δm^2) in two different neutrino flavor transition channels:

- Solar neutrino experiments (Homestake, Kamiokande, GALLEX/GNO, SAGE, Super-Kamiokande, SNO, BOREXino) measured $\nu_e \rightarrow \nu_\mu, \nu_\tau$ oscillations generated by $\Delta m_{\text{SOL}}^2 = 6.2_{-1.9}^{+1.1} \times 10^{-5} \text{ eV}^2$ and a mixing angle $\tan^2 \vartheta_{\text{SOL}} = 0.42_{-0.02}^{+0.04}$ [2]. The KamLAND experiment confirmed these oscillations by observing the disappearance of reactor $\bar{\nu}_e$ at an average distance of about 180 km. The combined fit of solar and KamLAND data leads to $\Delta m_{\text{SOL}}^2 = (7.6 \pm 0.2) \times 10^{-5} \text{ eV}^2$ and a mixing angle $\tan^2 \vartheta_{\text{SOL}} = 0.44 \pm 0.03$ [2].
- Atmospheric neutrino experiments (Kamiokande, IMB, Super-Kamiokande, MACRO, Soudan-2, MINOS) measured ν_μ and $\bar{\nu}_\mu$ disappearance through oscillations generated by $\Delta m_{\text{ATM}}^2 \simeq 2.3 \times 10^{-3} \text{ eV}^2$ and a mixing angle $\sin^2 2\vartheta_{\text{ATM}} \simeq 1$ [3]. The K2K and MINOS long-baseline experiments confirmed these oscillations by observing the disappearance of accelerator ν_μ at distances of about 250 km and 730 km, respectively. The MINOS data give $\Delta m_{\text{ATM}}^2 = 2.32_{-0.08}^{+0.12} \times 10^{-3} \text{ eV}^2$ and $\sin^2 2\vartheta_{\text{ATM}} > 0.90$ at 90% C.L. [4].

These measurements led to the current three-neutrino mixing paradigm, in which the three active neutrinos ν_e, ν_μ, ν_τ are superpositions of three massive neutrinos ν_1, ν_2, ν_3 with respective

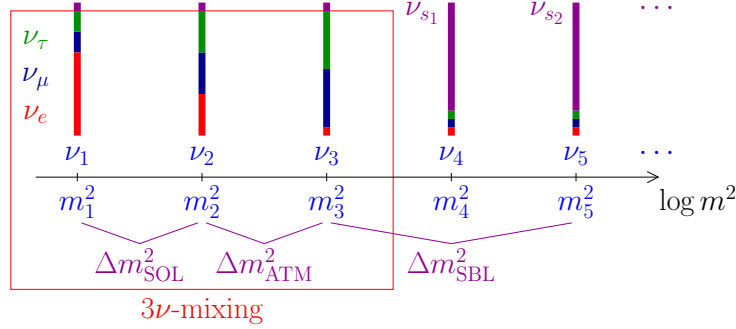


Figure 1. Schematic description of the neutrino spectrum beyond three-neutrino mixing with one or more relatively heavy additional massive neutrinos which are mainly sterile.

masses m_1, m_2, m_3 . The two measured squared-mass differences can be interpreted as

$$\Delta m_{\text{SOL}}^2 = \Delta m_{21}^2, \quad \Delta m_{\text{ATM}}^2 = |\Delta m_{31}^2| \simeq |\Delta m_{32}^2|, \quad (1)$$

with $\Delta m_{kj}^2 = m_k^2 - m_j^2$. In the standard parameterization of the 3×3 unitary mixing matrix (see Ref. [1]) $\vartheta_{\text{SOL}} \simeq \vartheta_{12}$, $\vartheta_{\text{ATM}} \simeq \vartheta_{23}$ and $\sin^2 \vartheta_{13} < 0.035$ at 90% C.L. [5].

The completeness of the three-neutrino mixing paradigm was challenged in 1995 by the observation of a signal of short-baseline $\bar{\nu}_\mu \rightarrow \bar{\nu}_e$ oscillations in the LSND experiment [6, 7], which would imply the existence of one or more squared-mass differences much larger than Δm_{SOL}^2 and Δm_{ATM}^2 . The MiniBooNE experiment was made in order to check the LSND signal with about one order of magnitude larger distance (L) and energy (E), but the same order of magnitude for the ratio L/E from which neutrino oscillations depend. The first results of the MiniBooNE experiment in neutrino mode did not show a signal compatible with that of LSND [8], but the results in antineutrino mode, presented in the summer of 2010 [9], show an excess of events over the background at approximately at the same L/E of LSND. This result revived the interest in the possibility of existence of one or more neutrinos with masses at the eV scale which can generate squared-mass differences for short-baseline oscillations.

Figure 1 illustrates schematically the neutrino spectrum beyond three-neutrino mixing with one or more additional massive neutrinos heavier than the three standard massive neutrinos. In the flavor basis the additional massive neutrinos correspond to sterile neutrinos, which do not have standard weak interactions and do not contribute to the number of active neutrinos determined by LEP experiments through the measurement of the invisible width of the Z boson, $N_a = 2.9840 \pm 0.0082$ [10]. The existence of sterile neutrinos which have been thermalized in the early Universe is compatible with Big-Bang Nucleosynthesis data [11, 12], with the indication however that schemes with more than one sterile neutrino are disfavored [13]. It is also compatible with cosmological measurements of the Cosmic Microwave Background and Large-Scale Structures if the neutrino masses are limited below about 1 eV [14–18]. Therefore, we consider neutrino mixing schemes in which the three standard neutrinos have masses much smaller than 1 eV and the additional neutrinos have masses at the eV scale. However, other sterile neutrinos may exist and the cosmological constraints can be avoided by suppressing the thermalization of sterile neutrinos in the early Universe and/or by considering non-standard cosmological theories. For example, a sterile neutrino with a mass scale much smaller than 1 eV could have important implications for solar neutrino oscillations (see Ref. [19]) and a sterile neutrino with a mass at the keV scale could constitute Warm Dark Matter (see Refs. [20, 21]).

A further indication in favor of short-baseline oscillations came from a new calculation of the reactor $\bar{\nu}_e$ flux presented in January 2011 [22] (see also Ref. [23]), which obtained an increase of about 3% with respect to the previous value adopted in the analysis of the data of reactor

| | 3+1 | 3+2 |
|---------------------------------|--------------------|--------------------|
| χ^2_{\min} | 100.2 | 91.6 |
| NDF | 104 | 100 |
| GoF | 59% | 71% |
| $\Delta m_{41}^2 [\text{eV}^2]$ | 0.89 | 0.90 |
| $ U_{e4} ^2$ | 0.025 | 0.017 |
| $ U_{\mu 4} ^2$ | 0.023 | 0.019 |
| $\Delta m_{51}^2 [\text{eV}^2]$ | | 1.61 |
| $ U_{e5} ^2$ | | 0.017 |
| $ U_{\mu 5} ^2$ | | 0.0061 |
| η | | 1.51π |
| $\Delta\chi^2_{\text{PG}}$ | 24.1 | 22.2 |
| NDF _{PG} | 2 | 5 |
| PGoF | 6×10^{-6} | 5×10^{-4} |

Table 1. Values of χ^2 , number of degrees of freedom (NDF), goodness-of-fit (GoF) and best-fit values of the mixing parameters obtained in our 3+1 and 3+2 fits of short-baseline oscillation data. The last three lines give the results of the parameter goodness-of-fit test [43]: $\Delta\chi^2_{\text{PG}}$, number of degrees of freedom (NDF_{PG}) and parameter goodness-of-fit (PGoF).

neutrino oscillation experiments. As illustrated in Fig. 2 of Ref. [24], the measured reactor rates are in agreement with those derived from the old $\bar{\nu}_e$ flux, but show a deficit of about 2.2σ with respect to the rates derived from the new $\bar{\nu}_e$ flux. This is the “reactor antineutrino anomaly” [25], which may be an indication in the $\bar{\nu}_e \rightarrow \bar{\nu}_e$ channel of a signal corresponding to the $\bar{\nu}_\mu \rightarrow \bar{\nu}_e$ signal observed in the LSND and MiniBooNE experiments. Finally, there is a “Gallium neutrino anomaly” [26–31], consisting in a short-baseline disappearance of electron neutrinos measured in the Gallium radioactive source experiments GALLEX [32] and SAGE [33].

In the following, I consider in Sections 2 and 3 the cases of 3+1 [34–37] and 3+2 [38–41] neutrino mixing, respectively, following the discussion in Ref. [42]. Conclusions are drawn in Section 4.

2. 3+1 Neutrino Mixing

In this Section I consider the simplest extension of three-neutrino mixing with the addition of one massive neutrino. In 3+1 neutrino mixing [34–37] the effective flavor transition and survival probabilities in short-baseline (SBL) experiments are given by

$$P_{\nu_\alpha \rightarrow \nu_\beta}^{\text{SBL}(-)(-)} = \sin^2 2\vartheta_{\alpha\beta} \sin^2 \left(\frac{\Delta m_{41}^2 L}{4E} \right), \quad P_{\nu_\alpha \rightarrow \nu_\alpha}^{\text{SBL}(-)(-)} = 1 - \sin^2 2\vartheta_{\alpha\alpha} \sin^2 \left(\frac{\Delta m_{41}^2 L}{4E} \right), \quad (2)$$

for $\alpha, \beta = e, \mu, \tau, s$ and $\alpha \neq \beta$, with

$$\sin^2 2\vartheta_{\alpha\beta} = 4|U_{\alpha 4}|^2 |U_{\beta 4}|^2, \quad \sin^2 2\vartheta_{\alpha\alpha} = 4|U_{\alpha 4}|^2 (1 - |U_{\alpha 4}|^2). \quad (3)$$

Therefore:

- (1) All effective SBL oscillation probabilities depend only on the absolute value of the largest squared-mass difference $\Delta m_{41}^2 = m_4^2 - m_1^2$.
- (2) All oscillation channels are open, each one with its own oscillation amplitude.
- (3) The oscillation amplitudes depend only on the absolute values of the elements in the fourth column of the mixing matrix, i.e. on three real numbers with sum less than unity, since the unitarity of the mixing matrix implies that $\sum_\alpha |U_{\alpha 4}|^2 = 1$.

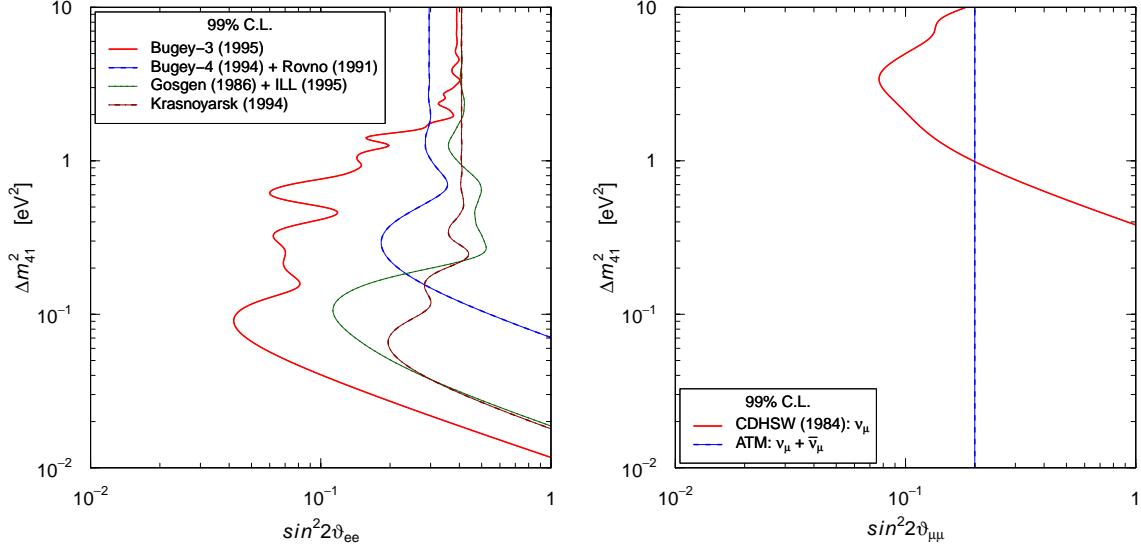


Figure 2. Exclusion curves obtained from the data of reactor $\bar{\nu}_e$ disappearance experiments (see Ref. [25]), from the data of the CDHSW ν_μ disappearance experiment [44], and from atmospheric neutrino data (extracted from the analysis in Ref. [40]).

- (4) CP violation cannot be observed in SBL oscillation experiments, even if the mixing matrix contains CP-violation phases, because neutrinos and antineutrinos have the same effective SBL oscillation probabilities. Hence, 3+1 neutrino mixing cannot explain the difference between neutrino [8] and antineutrino [9] oscillations observed in the MiniBooNE.

The dependence of the oscillation amplitudes in Eq. (3) on three independent absolute values of the elements in the fourth column of the mixing matrix implies that the amplitude of $\bar{\nu}_\mu \rightarrow \bar{\nu}_e$ transitions is limited by the absence of large SBL disappearance of $\bar{\nu}_e$ and $\bar{\nu}_\mu$ observed in several experiments.

The results of reactor neutrino experiments constrain the value $|U_{e4}|^2$ through the measurement of $\sin^2 2\vartheta_{ee}$. Even taking into account the reactor antineutrino anomaly [25] discussed in the Introduction, the $\bar{\nu}_e$ disappearance is small and large values of $\sin^2 2\vartheta_{ee}$ are constrained by the exclusion curves in the left panel of Fig. 2. Since values of $|U_{e4}|^2$ close to unity are excluded by solar neutrino oscillations (which require large $|U_{e1}|^2 + |U_{e2}|^2$), for small $\sin^2 2\vartheta_{ee}$ we have

$$\sin^2 2\vartheta_{ee} \simeq 4|U_{e4}|^2. \quad (4)$$

The value of $\sin^2 2\vartheta_{\mu\mu}$ is constrained by the curves in the right panel of Fig. 2, which have been obtained from the lack of ν_μ disappearance in the CDHSW ν_μ experiment [44] and from the requirement of large $|U_{\mu1}|^2 + |U_{\mu2}|^2 + |U_{\mu3}|^2$ for atmospheric neutrino oscillations [40]. Hence, $|U_{\mu4}|^2$ is small and

$$\sin^2 2\vartheta_{\mu\mu} \simeq 4|U_{\mu4}|^2. \quad (5)$$

From Eqs. (3), (4) and (5), for the amplitude of $\bar{\nu}_\mu \rightarrow \bar{\nu}_e$ transitions we obtain

$$\sin^2 2\vartheta_{e\mu} \simeq \frac{1}{4} \sin^2 2\vartheta_{ee} \sin^2 2\vartheta_{\mu\mu}. \quad (6)$$

Therefore, if $\sin^2 2\vartheta_{ee}$ and $\sin^2 2\vartheta_{\mu\mu}$ are small, $\sin^2 2\vartheta_{e\mu}$ is quadratically suppressed [34, 35]. This is illustrated in the left panel of Fig. 3, where one can see that the separate effects of the constraints on $\sin^2 2\vartheta_{ee}$ and $\sin^2 2\vartheta_{\mu\mu}$ exclude only the large- $\sin^2 2\vartheta_{e\mu}$ part of the region

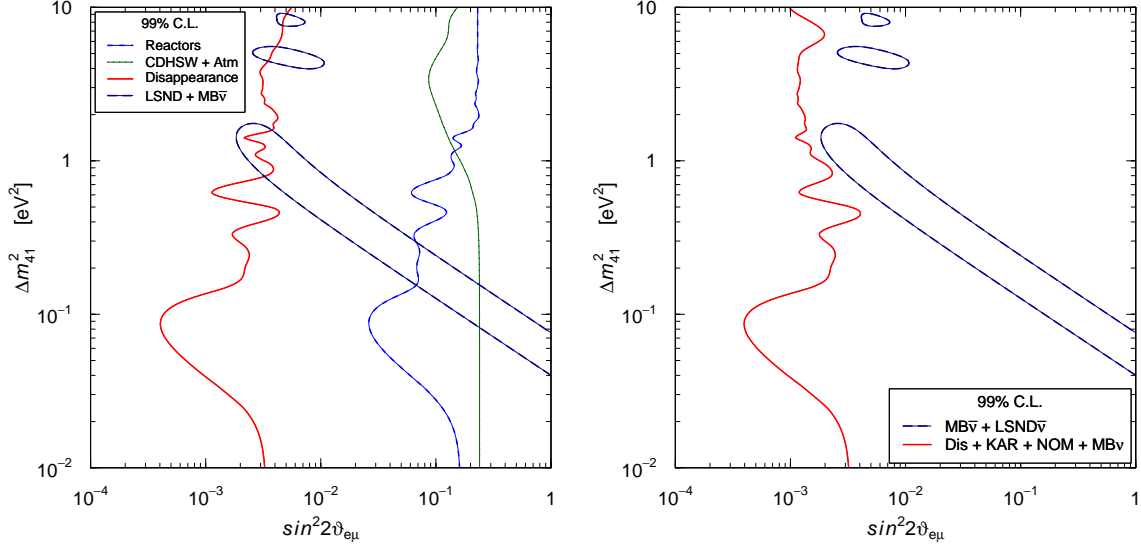


Figure 3. Left panel: Exclusion curves in the $\sin^2 2\vartheta_{e\mu}$ – Δm_{41}^2 plane obtained from the separate constraints in Fig. 2 (blue and green lines) and the combined constraint given by Eq. (6) (red line) from disappearance experiments (Dis). Right panel: Exclusion curve obtained with the addition of KARMEN [45] (KAR), NOMAD [46] (NOM) and MiniBooNE neutrino [8] ($\text{MB}\nu$) data (red line). In both panels the region enclosed by the dark-red lines is allowed by LSND and MiniBooNE antineutrino data.

allowed by LSND and MiniBooNE antineutrino data, whereas most of this region is excluded by the combined constraint in Eq. (6). As shown in the right panel of Fig. 3, the constraint becomes stronger by including the data of the KARMEN [45], NOMAD [46] and MiniBooNE neutrino [8] experiments, which did not observe a short-baseline $\bar{\nu}_\mu \rightarrow \bar{\nu}_e$ signal. Since the parameter goodness-of-fit [43] is 6×10^{-6} [42], 3+1 neutrino mixing is disfavored by the data. This conclusion has been reached recently in Refs. [42, 47–49] and confirms the pre-MiniBooNE antineutrino results in Refs. [34–37, 40, 41, 50].

However, in spite of the low value of the parameter goodness-of-fit it is not inconceivable to refuse to reject 3+1 neutrino mixing for the following reasons:

- (A) It is the simplest scheme beyond the standard three-neutrino mixing which can partially explain the data.
- (B) It corresponds to the natural addition of one new entity (a sterile neutrino) to explain a new effect (short-baseline oscillations). Better fits of the data require the addition of at least another new entity (in any case at least one sterile neutrino is needed to generate short-baseline oscillations).
- (C) The minimum value of the global χ^2 is rather good: $\chi_{\min}^2 = 100.2$ for 104 degrees of freedom.
- (D) There is a marginal appearance–disappearance compatibility: $\Delta\chi_{\text{PG}}^2 = 9.2$ with 2 degrees of freedom, corresponding to $\text{PGoF} = 1.0\%$.
- (E) 3+1 mixing is favored with respect to 3+2 mixing by the Big-Bang Nucleosynthesis limit $N_{\text{eff}} \leq 4$ at 95% C.L. obtained in Ref. [13].

Therefore, we consider the global fit of all data in the framework of 3+1 neutrino mixing, which yields the best-fit values of the oscillation parameters listed in Tab. 1.

Figure 4 shows the allowed regions in the $\sin^2 2\vartheta_{e\mu}$ – Δm_{41}^2 , $\sin^2 2\vartheta_{ee}$ – Δm_{41}^2 and $\sin^2 2\vartheta_{\mu\mu}$ – Δm_{41}^2 planes and the marginal $\Delta\chi^2$ ’s for Δm_{41}^2 , $\sin^2 2\vartheta_{e\mu}$, $\sin^2 2\vartheta_{ee}$ and $\sin^2 2\vartheta_{\mu\mu}$.

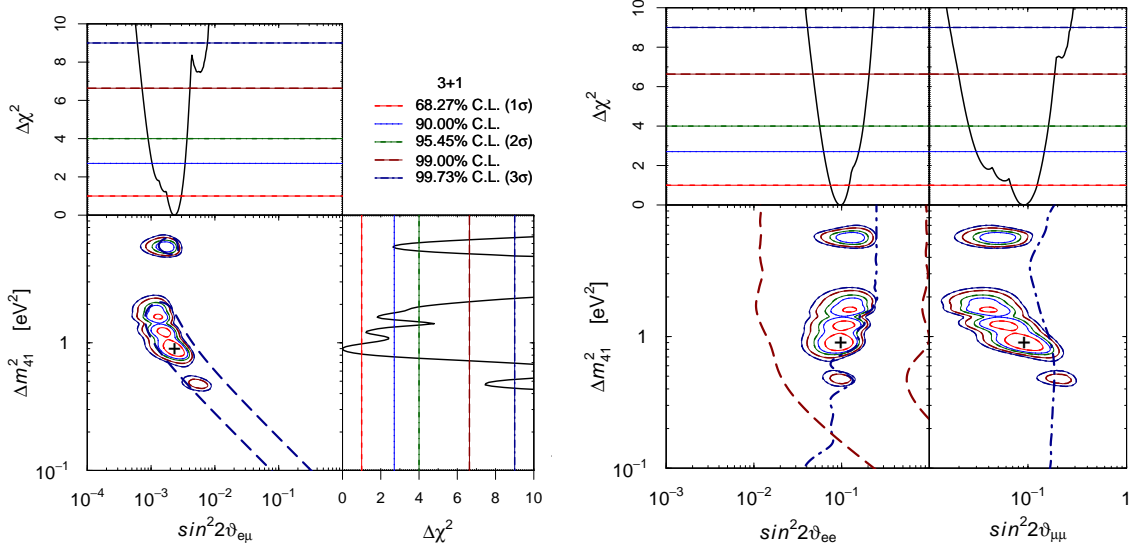


Figure 4. Allowed regions in the $\sin^2 2\vartheta_{e\mu}-\Delta m_{41}^2$, $\sin^2 2\vartheta_{ee}-\Delta m_{41}^2$ and $\sin^2 2\vartheta_{\mu\mu}-\Delta m_{41}^2$ planes and marginal $\Delta\chi^2$'s obtained from the global fit in 3+1 neutrino mixing. The best-fit point is indicated by a cross. Left panel: the isolated dark-blue long-dashed contours enclose the regions allowed at 3σ by the analysis of appearance data (LSND [7], KARMEN [45], NOMAD [46], MiniBooNE [8, 9]). Right panel: the isolated dark-blue dash-dotted lines are the 3σ exclusion curves obtained from reactor neutrino data and from CDHSW and atmospheric neutrino data. The isolated dark-red long-dashed lines delimit the region allowed at 99% C.L. by the Gallium anomaly [31].

3. 3+2 Neutrino Mixing

In 3+2 neutrino mixing [38–42, 47, 49] the relevant effective oscillation probabilities in short-baseline experiments are given by

$$P_{\nu_\mu \rightarrow \nu_e}^{\text{SBL}(-)} = 4|U_{\mu 4}|^2|U_{e 4}|^2 \sin^2 \phi_{41} + 4|U_{\mu 5}|^2|U_{e 5}|^2 \sin^2 \phi_{51} + 8\Omega \sin \phi_{41} \sin \phi_{51} \cos(\phi_{54}^{(+)} - \eta), \quad (7)$$

$$P_{\nu_\alpha \rightarrow \nu_\alpha}^{\text{SBL}(-)} = 1 - 4(1 - |U_{\alpha 4}|^2 - |U_{\alpha 5}|^2)(|U_{\alpha 4}|^2 \sin^2 \phi_{41} + |U_{\alpha 5}|^2 \sin^2 \phi_{51}) - 4|U_{\alpha 4}|^2|U_{\alpha 5}|^2 \sin^2 \phi_{54}, \quad (8)$$

for $\alpha, \beta = e, \mu$, with

$$\phi_{kj} = \Delta m_{kj}^2 L / 4E, \quad \Omega = |U_{\mu 4} U_{e 4} U_{\mu 5} U_{e 5}|, \quad \eta = \arg[U_{e 4}^* U_{\mu 4} U_{e 5} U_{\mu 5}^*]. \quad (9)$$

Note the change in sign of the contribution of the CP-violating phase η going from neutrinos to antineutrinos, which allows us to explain the CP-violating difference between MiniBooNE neutrino and antineutrino data.

Figure 5 shows the marginal allowed regions in the $\Delta m_{41}^2 - \Delta m_{51}^2$ plane obtained in our 3+2 global fit. The best-fit values of the mixing parameters are shown in Tab. 1.

The parameter goodness-of-fit obtained with the comparison of the fit of LSND and MiniBooNE antineutrino data and the fit of all other data is 5×10^{-4} . This is an improvement with respect to the 6×10^{-6} parameter goodness-of-fit obtained in 3+1 mixing. However, the value of the parameter goodness-of-fit remains low and the improvement is mainly due to the increased number of degrees of freedom, as one can see from Tab. 1. The persistence of a bad parameter goodness-of-fit is a consequence of the fact that the $\bar{\nu}_\mu \rightarrow \bar{\nu}_e$ transitions observed in LSND and MiniBooNE must correspond in any neutrino mixing scheme to enough short-baseline disappearance of $\bar{\nu}_e$ and $\bar{\nu}_\mu$ which has not been observed and there is an irreducible

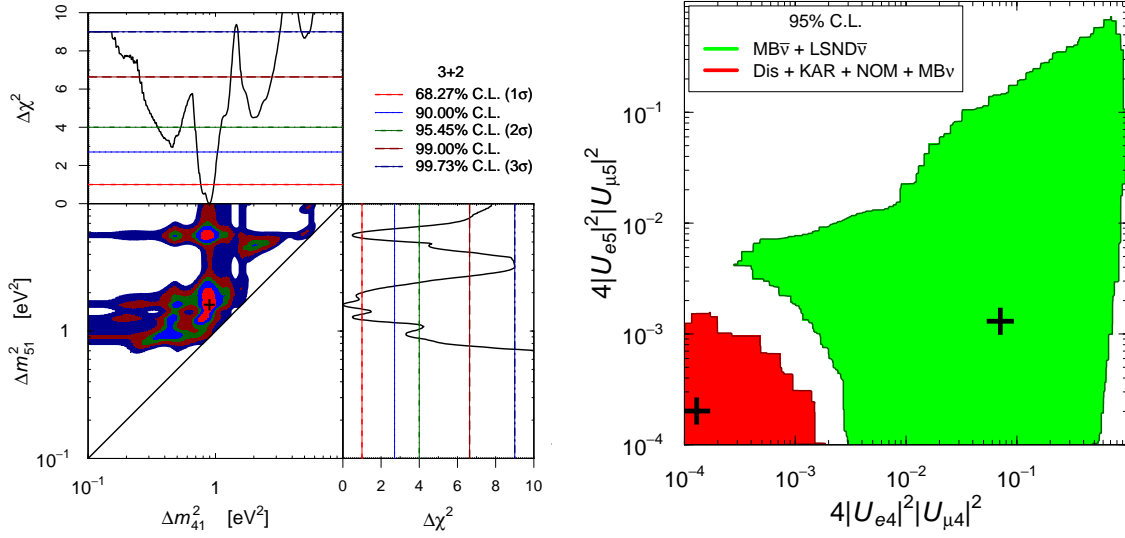


Figure 5. Left panel: allowed regions in the Δm_{41}^2 – Δm_{51}^2 plane and corresponding marginal $\Delta\chi^2$'s obtained from the global fit of all the considered data in 3+2 mixing. Right panel: comparison of the 95% C.L. allowed regions in the $4|U_{e4}|^2|U_{\mu 4}|^2$ – $4|U_{e5}|^2|U_{\mu 5}|^2$ plane obtained from LSND and MiniBooNE antineutrino data on the right (green area) and disappearance, KARMEN, NOMAD and MiniBooNE neutrino data on the left (red area). Best-fit points are indicated by crosses.

tension between the LSND and MiniBooNE antineutrino data and the KARMEN antineutrino data. The only benefit of 3+2 mixing with respect to 3+1 mixing is that they allow to explain the difference between MiniBooNE neutrino and antineutrino data through CP violation. In fact, neglecting the MiniBooNE neutrino data we obtain $\Delta\chi_{\text{PG}}^2 = 16.6$ with $\text{PGoF} = 3 \times 10^{-4}$ in 3+1 mixing and $\Delta\chi_{\text{PG}}^2 = 20.4$ with $\text{PGoF} = 1 \times 10^{-3}$ in 3+2 mixing. In this case $\Delta\chi_{\text{PG}}^2$ is even lower in 3+1 mixing than in 3+2 mixing!

The tension between LSND and MiniBooNE antineutrino data and disappearance, KARMEN, NOMAD and MiniBooNE neutrino data is illustrated in the right panel of Fig. 5, which is the analogue for 3+2 mixing of the right panel in Fig. 3 in 3+1 mixing. In practice, in order to show the tension in a two-dimensional figure we have marginalized the χ^2 over all the other mixing parameters, including the two Δm^2 's.

4. Conclusions

In the framework of 3+1 neutrino mixing, there is a strong tension between LSND and MiniBooNE antineutrino data and disappearance, KARMEN, NOMAD and MiniBooNE neutrino data [42, 47–49]. Since however the minimum value of the global χ^2 is rather good, one may choose to consider as possible 3+1 neutrino mixing, which can partially explain the data, taking into account its simplicity and the natural correspondence of one new entity (a sterile neutrino) with a new effect (short-baseline oscillations).

In the framework of 3+2 neutrino mixing the tension between LSND and MiniBooNE antineutrino data and disappearance, KARMEN, NOMAD and MiniBooNE neutrino data is reduced with respect to the 3+1 fit, but it is not eliminated (see the right panel of Fig. 5). Moreover, the improvement of the parameter goodness of fit with respect to that obtained in the 3+1 fit is mainly due to the increase of the number of oscillation parameters, as one can see from Tab. 1. Hence it seems mainly a statistical effect.

In conclusion, I think that the interpretation of the indications in favor of short-baseline oscillations is uncertain and new experiments are needed in order to clarify the reasons of the tensions in the data and for leading us to the correct interpretation.

References

- [1] Giunti C and Kim C W 2007 *Fundamentals of Neutrino Physics and Astrophysics* (Oxford, UK: Oxford University Press)
- [2] Abe K *et al.* (Super-Kamiokande) 2011 *Phys. Rev.* **D83** 052010 (*Preprint arXiv:1010.0118*)
- [3] Ashie Y *et al.* (Super-Kamiokande) 2005 *Phys. Rev.* **D71** 112005 (*Preprint hep-ex/0501064*)
- [4] Adamson P *et al.* (MINOS) 2011 *Phys. Rev. Lett.* **106** 181801 (*Preprint arXiv:1103.0340*)
- [5] Schwetz T, Tortola M and Valle J W F 2008 *New J. Phys.* **10** 113011 (*Preprint arXiv:0808.2016*)
- [6] Athanassopoulos C *et al.* (LSND) 1995 *Phys. Rev. Lett.* **75** 2650–2653 (*Preprint nucl-ex/9504002*)
- [7] Aguilar A *et al.* (LSND) 2001 *Phys. Rev.* **D64** 112007 (*Preprint hep-ex/0104049*)
- [8] Aguilar-Arevalo A A (MiniBooNE) 2009 *Phys. Rev. Lett.* **102** 101802 (*Preprint arXiv:0812.2243*)
- [9] Aguilar-Arevalo A A *et al.* (MiniBooNE) 2010 *Phys. Rev. Lett.* **105** 181801 (*Preprint arXiv:1007.1150*)
- [10] Schael S *et al.* (ALEPH, DELPHI, L3, OPAL, SLD, LEP Electroweak Working Group, SLD Electroweak Group, SLD Heavy Flavour Group) 2006 *Phys. Rept.* **427** 257 (*Preprint hep-ex/0509008*)
- [11] Cyburt R H, Fields B D, Olive K A and Skillman E 2005 *Astropart. Phys.* **23** 313–323 (*Preprint astro-ph/0408033*)
- [12] Izotov Y I and Thuan T X 2010 *Astrophys. J.* **710** L67–L71 (*Preprint arXiv:1001.4440*)
- [13] Mangano G and Serpico P D 2011 *Phys. Lett.* **B701** 296–299 (*Preprint arXiv:1103.1261*)
- [14] Hamann J, Hannestad S, Raffelt G G, Tamborra I and Wong Y Y 2010 *Phys. Rev. Lett.* **105** 181301 (*Preprint arXiv:1006.5276*)
- [15] Giusarma E *et al.* 2011 *Phys. Rev.* **D83** 115023 (*Preprint arXiv:1102.4774*)
- [16] Kristiansen J R and Elgaroy O 2011 (*Preprint arXiv:1104.0704*)
- [17] Hou Z, Keisler R, Knox L, Millea M and Reichardt C 2011 (*Preprint arXiv:1104.2333*)
- [18] Gonzalez-Morales A X, Poltis R, Sherwin B D and Verde L 2011 (*Preprint arXiv:1106.5052*)
- [19] de Holanda P C and Smirnov A Y 2011 *Phys. Rev.* **D83** 113011 (*Preprint arXiv:1012.5627*)
- [20] Kusenko A 2009 *Phys. Rept.* **481** 1–28 (*Preprint arXiv:0906.2968*)
- [21] Boyarsky A, Ruchayskiy O and Shaposhnikov M 2009 *Ann. Rev. Nucl. Part. Sci.* **59** 191–214 (*Preprint arXiv:0901.0011*)
- [22] Mueller T A *et al.* 2011 *Phys. Rev.* **C83** 054615 (*Preprint arXiv:1101.2663*)
- [23] Huber P 2011 *Phys. Rev.* **C84** 024617 (*Preprint arXiv:1106.0687*)
- [24] Giunti C 2011 La Thuile 2011, NeuTel 2011 and IFAE 2011 (*Preprint arXiv:1106.4479*)
- [25] Mention G *et al.* 2011 *Phys. Rev.* **D83** 073006 (*Preprint arXiv:1101.2755*)
- [26] Giunti C and Laveder M 2007 *Mod. Phys. Lett.* **A22** 2499–2509 (*Preprint hep-ph/0610352*)
- [27] Giunti C and Laveder M 2008 *Phys. Rev.* **D77** 093002 (*Preprint arXiv:0707.4593*)
- [28] Acero M A, Giunti C and Laveder M 2008 *Phys. Rev.* **D78** 073009 (*Preprint arXiv:0711.4222*)
- [29] Giunti C and Laveder M 2009 *Phys. Rev.* **D80** 013005 (*Preprint arXiv:0902.1992*)
- [30] Giunti C and Laveder M 2010 *Phys. Rev.* **D82** 053005 (*Preprint arXiv:1005.4599*)
- [31] Giunti C and Laveder M 2011 *Phys. Rev.* **C83** 065504 (*Preprint arXiv:1006.3244*)
- [32] Kaether F, Hampel W, Heusser G, Kiko J and Kirsten T 2010 *Phys. Lett.* **B685** 47–54 (*Preprint arXiv:1001.2731*)
- [33] Abdurashitov J N *et al.* (SAGE) 2009 *Phys. Rev.* **C80** 015807 (*Preprint arXiv:0901.2200*)
- [34] Okada N and Yasuda O 1997 *Int. J. Mod. Phys.* **A12** 3669–3694 (*Preprint hep-ph/9606411*)
- [35] Bilenky S M, Giunti C and Grimus W 1998 *Eur. Phys. J.* **C1** 247–253 (*Preprint hep-ph/9607372*)
- [36] Bilenky S M, Giunti C, Grimus W and Schwetz T 1999 *Phys. Rev.* **D60** 073007 (*Preprint hep-ph/9903454*)
- [37] Maltoni M, Schwetz T, Tortola M and Valle J 2004 *New J. Phys.* **6** 122 (*Preprint hep-ph/0405172*)
- [38] Sorel M, Conrad J and Shaevitz M 2004 *Phys. Rev.* **D70** 073004 (*Preprint hep-ph/0305255*)
- [39] Karagiorgi G *et al.* 2007 *Phys. Rev.* **D75** 013011 (*Preprint hep-ph/0609177*)
- [40] Maltoni M and Schwetz T 2007 *Phys. Rev.* **D76** 093005 (*Preprint arXiv:0705.0107*)
- [41] Karagiorgi G, Djurcic Z, Conrad J, Shaevitz M H and Sorel M 2009 *Phys. Rev.* **D80** 073001 (*Preprint arXiv:0906.1997*)
- [42] Giunti C and Laveder M 2011 (*Preprint arXiv:1107.1452*)
- [43] Maltoni M and Schwetz T 2003 *Phys. Rev.* **D68** 033020 (*Preprint hep-ph/0304176*)
- [44] Dydak F *et al.* (CDHSW) 1984 *Phys. Lett.* **B134** 281
- [45] Armbruster B *et al.* (KARMEN) 2002 *Phys. Rev.* **D65** 112001 (*Preprint hep-ex/0203021*)
- [46] Astier P *et al.* (NOMAD) 2003 *Phys. Lett.* **B570** 19–31 (*Preprint hep-ex/0306037*)
- [47] Akhmedov E and Schwetz T 2010 *JHEP* **10** 115 (*Preprint arXiv:1007.4171*)
- [48] Giunti C and Laveder M 2011 *Phys. Rev.* **D83** 053006 (*Preprint arXiv:1012.0267*)
- [49] Kopp J, Maltoni M and Schwetz T 2011 *Phys. Rev. Lett.* **107** 091801 (*Preprint arXiv:1103.4570*)
- [50] Maltoni M, Schwetz T, Tortola M A and Valle J W F 2002 *Nucl. Phys.* **B643** 321–338 (*Preprint hep-ph/0207157*)